Journal of Cellular Biochemistry 89:191–202 (2003)

Sequence Requirement for Nuclear Localization and Growth Inhibition of $p27^{Kip1R}$, a Degradation-Resistant Isoform of $p27^{Kip1}$

Katsuya Hirano, Ying Zeng, Mayumi Hirano, Junji Nishimura, and Hideo Kanaide*

Division of Molecular Cardiology, Research Institute of Angiocardiology, Graduate School of Medical Sciences, Kyushu University 3-1-1 Maidashi, Higashi-ku, Fukuoka 812-8582, Japan

Abstract $p27^{Kip1R}$ is an isoform of $p27^{Kip1}$, having a distinct C-terminus. The sequences of $p27^{Kip1R}$ required for nuclear localization and growth inhibition were determined in HeLa cells using a green fluorescence protein (GFP) as a reporter molecule. Region 153–168 and residues K168 and I169 were determined to play a critical role in the nuclear localization of $p27^{Kip1R}$. Aliphatic amino acid was found to be a substitute for the basic residue in the typical nuclear localization signal, while its functional substitution was incomplete, thereby causing a significant cytoplasmic retention of $p27^{Kip1R}$. $p27^{Kip1R}$ is thus the first example of an atypical bipartite nuclear localization signal with aliphatic amino acid as a functional residue. Despite cytoplasmic retention, $p27^{Kip1R}$ inhibited the cell growth as well as $p27^{Kip1}$, while GFP alone had no effect. The mutants lacking an N-terminus containing the binding regions for cyclins and cyclin-dependent kinases also showed a significant degree of nuclear localization, but failed to inhibit cell growth. The growth inhibition by $p27^{Kip1R}$ as well as $p27^{Kip1}$ was thus suggested to originate in the common N-terminal region. J. Cell. Biochem. 89: 191–202, 2003.

Key words: $p27^{Kip1}$; isoform; nuclear localization signal; green fluorescent protein; growth inhibition

$p27^{Kip1}$ is one of the cyclin-dependent kinase (Cdk) inhibitors, and causes growth arrest in response to such anti-mitogenic signals as serum deprivation and cell–cell contact [Sherr and Roberts, 1995; Hirano et al., 2001b]. The signal required for the nuclear localization of $p27^{Kip1}$ is considered to be in the C-terminal region [Polyak et al., 1994; Toyoshima and Hunter, 1994], and we previously reported that residues 153–166 are the minimal sequence required for significant nuclear localization, while four basic residues (K153, R154, K165, R166), especially R166, play a critical role in the nuclear localization [Zeng et al., 2000]. The minimal sequence required for the nuclear localization of $p27^{Kip1}$ thus closely correlates with the classical bipartite nuclear localization signal (NLS) [Kalderon et al., 1984; Conti et al., 1998]. We have cloned an isoform of $p27^{Kip1}$, hence referred to as $p27^{Kip1R}$, which has a distinct C-terminus of 18 residues and is resistant to proteasome-mediated degradation [Hirano et al., 2001a]. $p27^{Kip1R}$ becomes divergent at residue 163 (see Fig. 4), and thus lacks a part of the bipartite NLS and a putative Cdk-phosphorylation site (T187) seen in $p27^{Kip1}$ [Polyak et al., 1994; Zeng et al., 2000; Hirano et al., 2001a]. We previously reported that $p27^{Kip1R}$ mainly localizes to the nucleus despite a partial defect in the classical NLS [Hirano et al., 2001a]. In addition to the nuclear localization, $p27^{Kip1R}$ demonstrated some retention in the cytosol, which is in contrast to the exclusive nuclear localization seen with

Grant sponsor: Ministry of Education, Culture, Sports, Science and Technology, Japan; Grant sponsor: Ministry of Health, Labour and Welfare, Japan; Grant sponsor: NOVARTIS Foundation, Japan; Grant sponsor: Japan Space Forum; Grant sponsor: Mochida Memorial Foundation.

*Correspondence to: Prof. Hideo Kanaide, MD, PhD, Division of Molecular Cardiology, Research Institute of Angiocardiology, Graduate School of Medical Sciences, Kyushu University 3-1-1 Maidashi, Higashi-ku, Fukuoka 812-8582, Japan.
E-mail: kanaide@molcar.med.kyushu-u.ac.jp

Received 4 October 2002; Accepted 14 January 2003
DOI 10.1002/jcb.10499

$p27^{Kip1}$ [Hirano et al., 2001a]. A previous study suggested that NLS of $p27^{Kip1R}$ is also in a bipartite configuration [Hirano et al., 2001a]. However, further analyses are needed to elucidate the mechanism of subcellular localization in $p27^{Kip1R}$.

The N-terminal region common to $p27^{Kip1}$ and $p27^{Kip1R}$ contains binding sites for cyclin and Cdk [Russo et al., 1996], thus suggesting that this region plays an important role in the growth inhibition. In fact, $p27^{Kip1R}$ as well as $p27^{Kip1}$ was shown to cause G_1 arrest and growth inhibition [Hirano et al., 2001a]. On the other hand, nuclear localization is a prerequisite for the Cdk inhibitors to function as a cell cycle regulator. The subcellular localization of $p27^{Kip1R}$ was shown to be distinct from $p27^{Kip1}$ [Zeng et al., 2000; Hirano et al., 2001a]. Furthermore, $p27^{Kip1}$ was shown to induce not only growth arrest but also cell scattering and filopodia formation in HepG2, and the latter effects were attributed to the C-terminal half of the molecule [Nagahara et al., 1998]. The mechanism and sequence requirements of the growth inhibition might thus differ between the two isoforms. However, they remain to be determined in $p27^{Kip1R}$.

In the present study, we utilized a green fluorescence protein (GFP) as a reporter molecule and determined the sequences of $p27^{Kip1R}$ required for nuclear localization and growth inhibition, in comparison with those of $p27^{Kip1}$. The nuclear localization was quantitatively evaluated using a fluorescence image obtained with a confocal laser scanning microscope as previously described [Zeng et al., 2000]. The effects of $p27^{Kip1R}$ and its mutants on the cell growth were examined by transiently transfecting them to HeLa cells, and then the growth rates of the fluorescence-positive and negative cells were separately evaluated. We herein demonstrated the first example of an atypical bipartite nuclear localization signal with an aliphatic amino acid as a functional residue in $p27^{Kip1R}$.

METHODS

Cell Culture

HeLa cells were cultured in Dulbecco's modified Eagle medium (DMEM, Life Technologies, Rockville, MD) supplemented with 10% fetal bovine serum, 100 U/ml penicillin, 100 μg/ml streptomycin as described previously [Hirano et al., 2001a]. For confocal microscopic observations, the cells were seeded on glass coverslips placed in 35-mm dishes.

Plasmid Construction

A plamsid pEGFP-N1 (Clontech, Palo Alto, CA) was used to express a fusion protein with GFP at the C-terminus in the mammalian cells as described [Zeng et al., 2000; Hirano et al., 2001a]. The plasmids, pEGFP-Kip1(1–198) and pEGFP-Kip1R(16–180), expressing a wild type full-length $p27^{Kip1}$ (198 amino acids) and a region corresponding to residues 16–180 of $p27^{Kip1R}$, respectively, were as previously described [Zeng et al., 2000; Hirano et al., 2001a]. Because of the lack of the N-terminal, 8 residues in the original clone of $p27^{Kip1R}$ [Hirano et al., 2001a], the second methionine, M16, was used as an initiation codon in the expression with pEGFP-N1 plasmid. Kip1(1–165), Kip1(1–166), Kip1(152–198), Kip1(153–198), Kip1(154–198), and Kip1(152–166), the truncation mutants of Kip1 encoding the residues indicated in the parenthesis, and $Kip1(1–198)^{R166A}$, Kip1 (1–198) containing a site-directed mutation of R166 to A, are as previously described [Zeng et al., 2000]. A truncation mutant Kip1/KipR(16–162) containing a sequence common to $p27^{Kip1}$ and $p27^{Kip1R}$ is as previously described [Hirano et al., 2001a]. The cDNAs for the additional truncation mutants of Kip1(1–198) and Kip1R(16–180) used in the present study were obtained by PCR with the clones of the porcine $p27^{Kip1}$ (Accession No. AB031955) and $p27^{Kip1R}$ (Accession No. AB031958) as template, respectively. The site-directed mutations were introduced by using the overlap extension PCR technique [Ho et al., 1989; Zeng et al., 2000]. The PCR products containing the intended mutations were ligated to the *Eco*RI and *Bam*HI sites of pEGFP-N1. The newly constructed truncation mutants are Kip1(1–169), Kip1(152–169), Kip1(153–169), Kip1R(16–167), Kip1R(16–168), Kip1R(16–170), Kip1R(152–180), Kip1R(153–180), Kip1R (154–180), and Kip1R(155–180). The newly constructed site-directed mutants are $Kip1(1–198)^{R166I}$, $Kip1(1–198)^{R169A}$, $Kip1R(16–180)^{I169R}$, $Kip1R(16–180)^{I169A}$, $Kip1R(16–180)^{K168A}$, and $Kip1R(16–180)^{K168A+I169A}$. The plasmid DNA used for transfection was purified with a plasmid purification kit (Qiagen, Hilden, Germany). All constructs were confirmed to contain no un-intended mutations by

determining DNA sequences on an ABI PRISM 310 Genetic Analyzer (Perkin-Elmer, Foster City, CA).

Transfection of Cells With Expression Plasmid

The cells were seeded on the day before transfection. After rinsing with DMEM, the cells were transfected by incubation in 1 ml DMEM containing 10 μg LipofectAMINE (Life Technologies, Rockville, MD) and 1 μg plasmid DNA at 37°C for 5 h. LipofectAMINE and plasmid DNA had been incubated in 200 μl DMEM at room temperature for 15 min before transfection. After 5-h incubation, the transfection mixture was replaced with 10% serum-containing complete growth media, and the cell culture was resumed. In the preliminary experiments, 5 h exposure to 1 μg/ml plasmid DNA and 10 μg/ml LipofectAMINE was determined to be optimal transfection conditions to obtain higher transfection rate and lower toxicity in HeLa cells (data not shown).

Flow Cytometric Determination of Transfection Rate

The transfection rate (a percentage of GFP fluorescence positive cells) was determined on a flow cytometer (FACSCalibur; Becton Dickinson, San Jose, CA). The cells were harvested by trypsin treatment, and then were suspended in PBS at a density of approximately $1-10 \times 10^5$ cells/ml. The fluorescence of GFP was detected by 488-nm laser excitation and FL1 detector with a detection range of 515–545 nm. A program Cell Quest ver.3.2.1 (Beckton Dickinson) was used to determine a fraction of the GFP fluorescence-positive cells on a dot plot presentation of data with the fluorescence intensity values on the abscissa (FL1) and the forward scatter values on the ordinate (FSC). The border between the GFP-positive and negative populations was determined so as to include all untransfected negative control cells in the negative population.

When the cells were fixed in 50% methanol for staining with propidium iodide as described [Hirano et al., 2001a,b], the GFP fluorescence disappeared from the cell, thus indicating a loss of the recombinant protein. Therefore, we did not perform a simultaneous determination of the cell cycle profile and the GFP fluorescence.

Analysis of Cell Growth

HeLa cells were seeded at 60,000 cells per 35-mm diameter culture dish (Nunc, Copenhagen, Denmark) on the day before transfection. The cells were then transfected as described above. After the incubation with a transfection mixture, the cells were washed in growth medium containing 10% serum, and then the culture was resumed. At the indicated time point after the transfection, the cells were harvested by trypsin treatment. Since the cell sorting does not give quantitative estimation of the total number of the GFP-positive and negative cells in one dish [Hirano et al., 2001a], we estimated the cell growth of the GFP-positive and negative cells as follows. The total cell number including both GFP-positive and negative cells was determined on a hemocytometer, and then the cells were subjected to flow cytometry to determine the transfection rate as described above. According to the transfection rate, the number of the GFP-positive and negative cells were estimated from the total cell number, and the growth curves for the GFP-positive and negative cells were thus separately constructed.

Confocal Fluorescence Microscopy

The cells on the glass coverslips were fixed in 2% paraformaldehyde at room temperature for 5 min on the next day of the transfecion. After washing three times with phosphate-buffered saline, coverslips were mounted on glass slides and sealed with nail oil. The image of the GFP fluorescence was observed under a laser scanning microscopy LSM GB200 (Olympus, Tokyo, Japan), using a 60× objective lens, 488-nm laser excitation, and a 500–530 band pass emission filter. Fluorescence images were obtained at the nuclear level, and saved as TIFF files to create representative photos and to perform quantitative analyses.

Quantitation of Fluorescence Ratio of Cytoplasm to Nucleus

The mean fluorescence intensity of a certain area of the cytoplasm and nucleus in the same cells was determined on a fluorescence image using a computer program NIH Image ver.1.6.2 (National Institute of Health, Besethda, MD). The fluorescence ratio (cytoplasm/nucleus) was determined for each cell to quantitatively evaluate the nuclear localization as described previously [Zeng et al., 2000]. Since a confocal

fluorescence image was a slice with a certain depth, the mean fluorescence intensity for a certain area reflects the mean concentration of the GFP protein. Therefore, the ratio of cytosolic to nuclear amount can be estimated by the fluorescence ratio [Zeng et al., 2000]. The average fluorescence ratio was obtained from at least 10 different cells for each construction.

Western Blot Analysis of Expression of the Recombinant Proteins in HeLa Cells

The cells were harvested with trypsin treatment 24 h after transfection and the transfection rate was determined with a flow cytometer as described above. Then, the cell lysate was prepared in RIPA buffer (50 mM Tris-HCl, pH 7.2, 1% Triton X-100, 0.5% sodium deoxycholate, 0.1% SDS, 500 mM NaCl, 10 mM $MgCl_2$, 10 μg/ml leupeptin, 10 μg/ml aprotinin, 10 μM μM 4-aminidophenylmethane sulfonyl fluoride). Twenty-microgram total cellular protein was separated by sodium dodecy sulfate–polyacrylamide gel electrophoresis (SDS–PAGE) on 15% gel, followed by transfer to polyvinylidene difluoride membrane. The GFP fusion protein was detected using a rabbit polyclonal anti-GFP antibody (Clontech, Palo Alto, CA), a horseradish peroxidase-conjugated secondary antibody (Vector Laboratories, Burlingame, CA), and enhanced chemiluminescence technique (Amersham Pharmacia Biotech, Buckinghamshire, UK). The density of the band was determined using a computer program NIH image ver. 1.6.2 after obtaining a chemiluminescence image with a CCD camera (Atto, Tokyo, Japan). The molar expression level of the recombinant protein was estimated from the density data by adjusting them according to the transfection rate and molecular weight. The relative expression level of each construct was determined by comparing to the mean expression level obtained with the constructs of $p27^{Kip1}$ and $p27^{Kip1R}$.

Statistical Analysis

Student's *t*-test was used to determine any statistically significant differences. $P < 0.05$ was considered to be statistically significant.

RESULTS

Region Required for the Significant Nuclear Localization of $p27^{Kip1R}$

The series of truncation mutants of $p27^{Kip1R}$ was constructed to determine the region required for the nuclear localization of $p27^{Kip1R}$. Kip1R(16–180) localized mostly in the nucleus (Fig. 1a), with a slight but significant retention in the cytoplasm (Fig. 1b). Kip1/Kip1R(16–162), a mutant containing the sequences common to $p27^{Kip1}$ and $p27^{Kip1R}$, showed a fluorescence distribution similar to that seen with GFP alone (Fig. 1a), and there was no statistically significant difference in the fluorescence ratio between Kip1/Kip1R(16–162) and GFP alone (Fig. 1b), suggesting a complete loss of significant nuclear localization. The extension of 6 residues or more to the C-terminus, Kip1R(16–168) and Kip1R(16–170), but not the extension of 5 residues, Kip1R(16–167), was required to induce a significantly lower degree of cytoplasmic distribution, namely, a significantly higher degree of nuclear localization than that seen with GFP alone (Fig. 1a,b). However, the nuclear localization of both Kip1R(16–168) and Kip1R(16–170) was greatly impaired in comparison to that seen with Kip1R(16–180) (Fig. 1b). On the other hand, the N-terminal deletion of 1–153 and more, Kip1R(154-180) and Kip1R(155-180), caused a similar distribution to that seen with GFP alone, while Kip1R(153-180) demonstrated a significantly lower degree of cytoplasmic distribution (Fig. 1). However, the nuclear localization was more greatly impaired in Kip1R(153–180) than in Kip1(153–198), a corresponding mutant of $p27^{Kip1}$, which retained almost the full activity of NLS (Fig. 2). As a result, the region 153–168 was required to obtain significant nuclear localization of $p27^{Kip1R}$.

Requirement of R169 for the Full Activity of NLS in $p27^{Kip1}$

Kip1(1–198) exclusively localized in the nucleus (Fig. 2a), and the truncation of the region 166–198, Kip1(1–165), caused a similar distribution to that seen with GFP alone (Fig. 2a). An addition of one residue, Kip1(1–166), caused cytoplasmic distribution to the extent significantly lower than that seen with GFP alone, but still significantly higher than that seen with Kip1(1–198) (Fig. 2b). The extension of three more residues to the C-terminus, Kip1(1–169), exclusively localized in the nucleus (Fig. 2a), and the fluorescence ratio did not significantly differ from Kip1(1–198) (Fig. 2b). On the other hand, a deletion of 1–153, Kip1(154–198), caused a similar distribution pattern to that seen with GFP alone (Fig. 2).

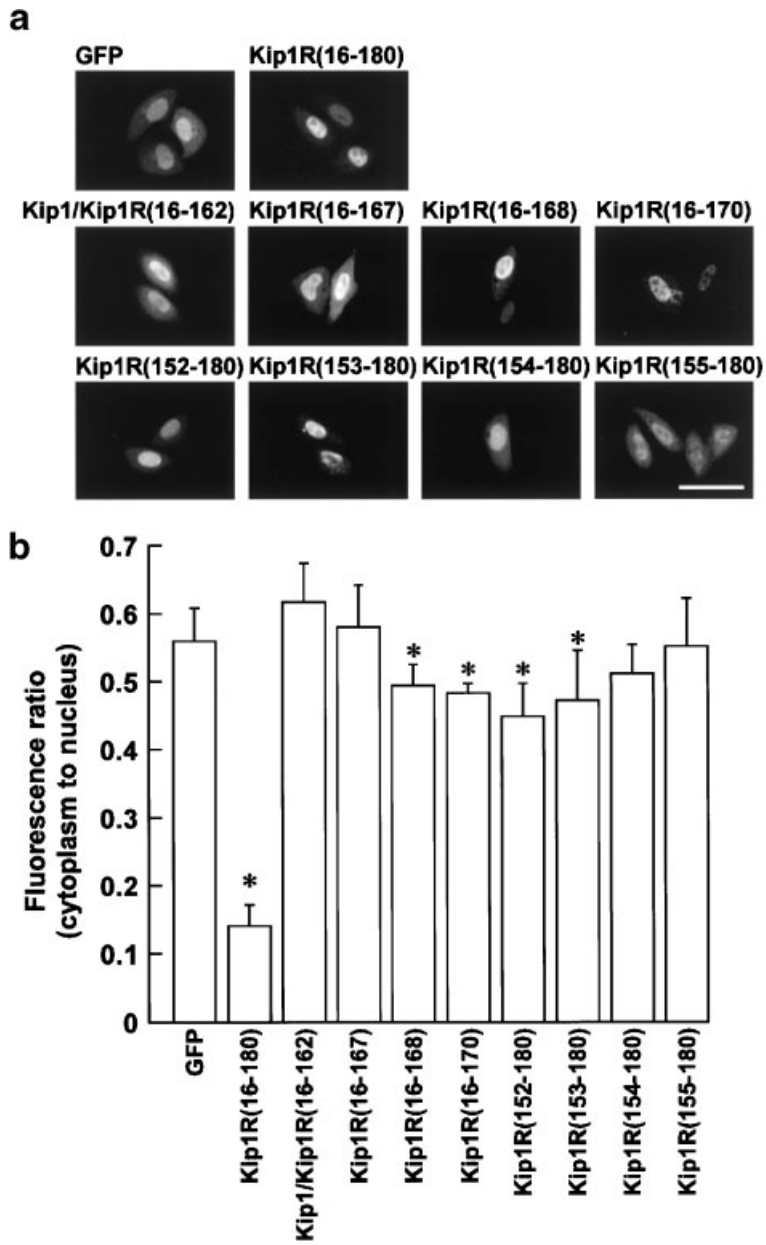

Fig. 1. Subcellular localization of $p27^{Kip1R}$ and its truncated mutants in HeLa cells. **a**: Representative photos of a confocal image showing the GFP fluorescence of $p27^{Kip1R}$ and its truncated mutants. GFP, GFP tag alone; Kip1R(16–180), $p27^{Kip1R}$ lacking the N-terminal 15 residues and thus containing residues 16–180; Kip1/KipR(16–162), a truncation mutant containing the residues 16–162, common to $p27^{Kip1}$ and $p27^{Kip1R}$. The amino acid residues at the N-terminal and C-terminal end of the truncated mutants are indicated in parentheses. Scale bar, 50 μm. **b**: A quantitative evaluation of the nuclear localization of each construct by the ratio of the fluorescence intensity in the cytosol to that in the nucleus. The data are the mean ± SEM of 10 different cells. $^*P < 0.05$ compared with the GFP alone.

Kip1(153–198) and Kip1(152–198) were both exclusively localized in the nucleus (Fig. 2a), and the fluorescence ratio did not significantly differ from that obtained with Kip1(1–198) (Fig. 2b). The region 153–169 is thus required to achieve a full activity of NLS, while the region 153–166 is the minimal sequence required to obtain a significant degree of nuclear localization, as previously reported [Zeng et al., 2000].

A further analysis of truncation mutants added support to the evidence that the region 153–169 was necessary for the full activity of the NLS in $p27^{Kip1}$. Kip1(152–166) showed a

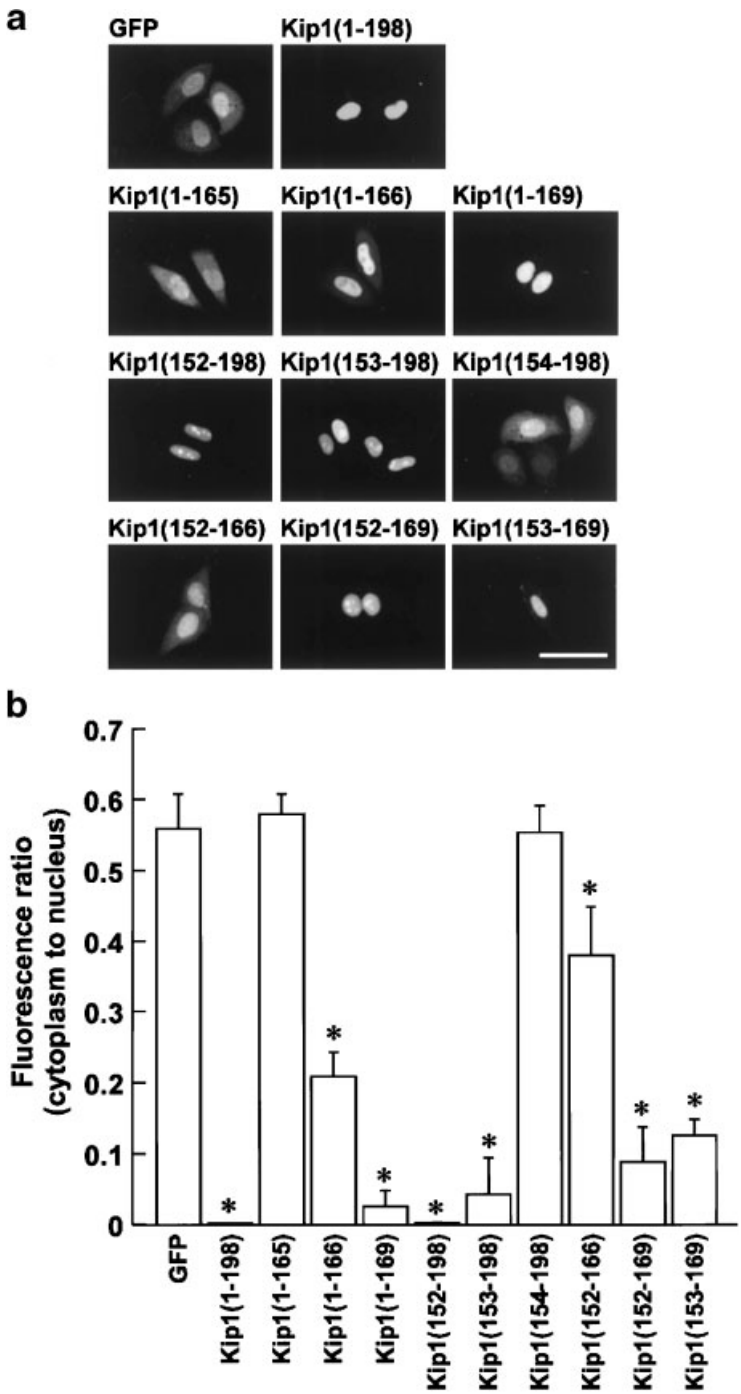

Fig. 2. Subcellular localization of $p27^{Kip1}$ and its truncated mutants in HeLa cells. **a**: Representative photos of a confocal image showing GFP fluorescence of $p27^{Kip1}$ and its truncated mutants. GFP, GFP tag alone; Kip1(1–198), wild type $p27^{Kip1}$ containing 198 amino acids full length. The amino acid residues at the N-terminal and C-terminal end of the truncated mutants are indicated in parentheses. Scale bar, 50 μm. **b**: A quantitative evaluation of the nuclear localization of each construct by the ratio of the fluorescence intensity in the cytosol to that in the nucleus. The data are the mean ± SEM of 10 different cells. $^*P < 0.05$ compared with the GFP alone.

substantially high level of cytoplasmic distribution (Fig. 2b) as previously reported [Zeng et al., 2000]. On the other hand, the truncation mutants including R169, Kip1(152–169), and Kip1(153–169), exclusively localized to the nucleus (Fig. 2a), although a statistical analysis revealed a significant degree of cytoplasmic distribution (Fig. 2b). However, it was much

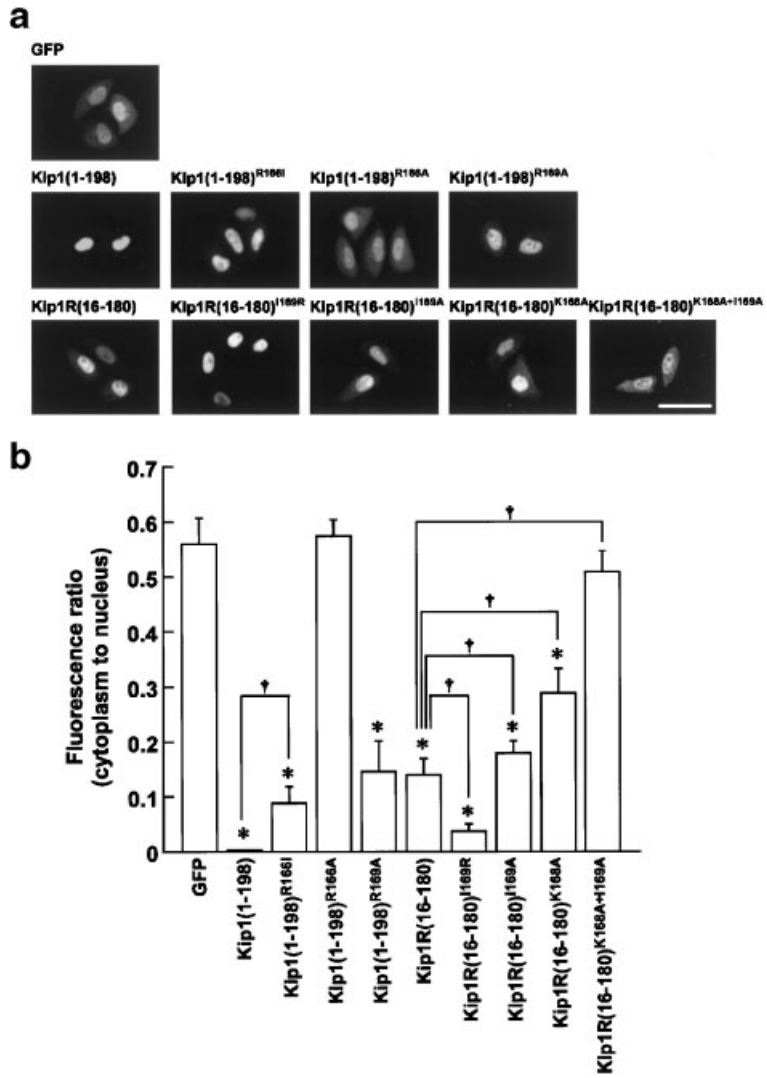

Fig. 3. Subcellular localization of $p27^{Kip1}$, $p27^{Kip1R}$, and their site-directed mutants in HeLa cells. **a**: Representative photos of a confocal image showing GFP fluorescence of $p27^{Kip1}$, $p27^{Kip1R}$, and their site-directed mutants. GFP, Kip1(1–198), and Kip1R(16–180), same as in Figures 1 and 2. $Kip1(1–198)^{R166I}$, $Kip1(1–198)^{R166A}$, and $Kip1(1–198)^{R169A}$, a full-length $p27^{Kip1}$ containing a site-directed mutation of R166 to I, R166 to A and R169 to A, respectively. $Kip1R(16–180)^{I169R}$, $Kip1R(16–180)^{I169A}$, $Kip1R(16–180)^{K168A}$ and $Kip1R(16–180)^{K168A+I169A}$, Kip1R(16–180) containing site-directed mutations of I169 to R, I169 to A, K168 to A, and both K168 and I169 to A, respectively. Scale bar, 50 μm. **b**: A quantitative evaluation of the nuclear localization of each construct by the ratio of the fluorescence intensity in the cytosol to that in the nucleus. The data are the mean ± SEM of 10 different cells. $^{\dagger}P < 0.05$; $^{*}P < 0.05$ compared with the GFP alone.

weaker than that observed with Kip1(152–166) and similar to that seen with Kip1(153–198) (Fig. 2a,b). An analysis of the site-directed mutation further supported the significant role of R169 in nuclear localization of $p27^{Kip1}$ (Fig. 3). A mutation of R169 to A caused a significantly higher degree of cytoplasmic distribution (Fig. 3b). However, $Kip1(1–198)^{R166A}$ caused a similar distribution pattern to that seen with GFP alone, namely, a complete loss of the nuclear localization (Fig. 3b).

Importance of Aliphatic Amino Acid in the Nuclear Localization of $p27^{Kip1R}$

The minimal sequences required for the significant nuclear localization of $p27^{Kip1R}$ do not perfectly match the consensus sequence of a bipartite NLS [Kalderon et al., 1984; Conti et al., 1998]. There is only one basic amino acid in the C-terminal region specific to $p27^{Kip1R}$ (Fig. 6). A comparison of the sequences between $p27^{Kip1}$ and $p27^{Kip1R}$ (Fig. 6) suggested that residues

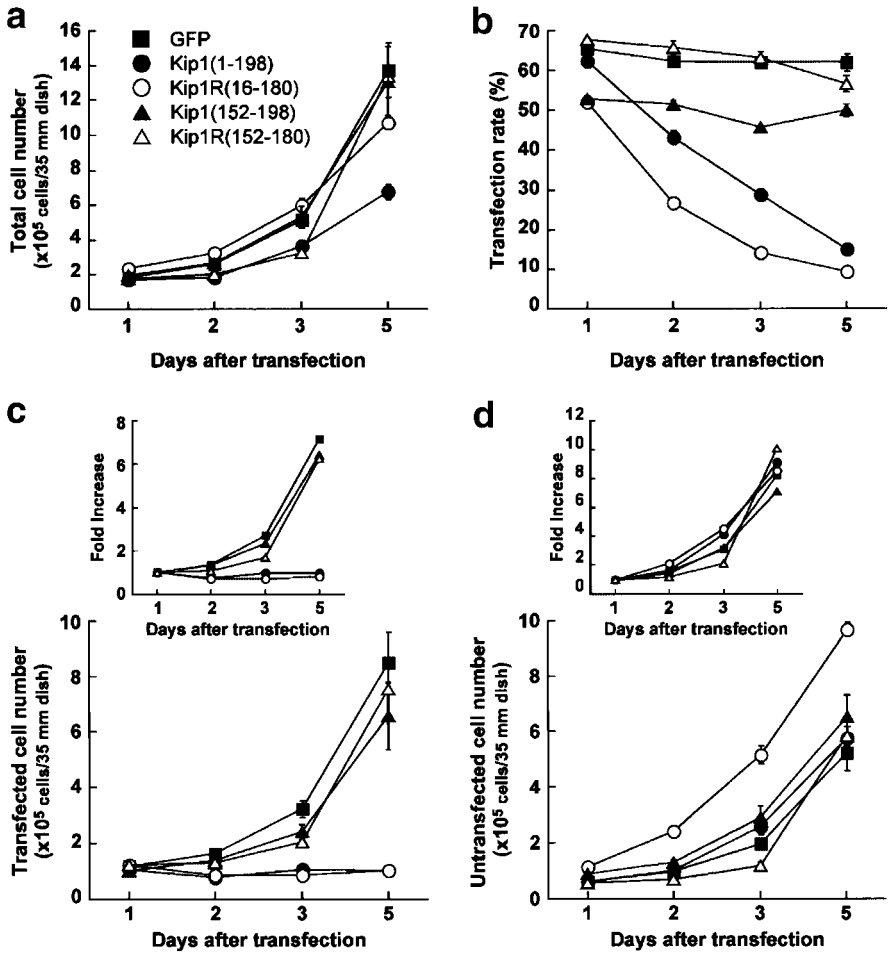

Fig. 4. Inhibition of the cell growth by $p27^{Kip1}$ and $p27^{Kip1R}$. The changes in the total cell count (**a**) and the transfection rate (**b**) after the transient transfection with GFP alone, and GFP-tagged Kip1(1–198), Kip1R(16–180), Kip1(152–198), and Kip1R(152–180) are shown. Based on the total cell count and the transfection rate, the growth curves for the expression-positive (**c**) and negative (**d**) cells were separately constructed. The data are the mean ± SEM (n = 3). The insets show the fold increase in the mean cell number while assigning the mean cell number on day 1 to be 1.0.

K168–I169 in $p27^{Kip1R}$ correspond to residues K165–R166 in $p27^{Kip1}$, as the residues containing the first basic amino acid following the spacer region of a bipartite NLS. The mutation of I169 to R in $p27^{Kip1R}$, $Kip1R(16–180)^{I169R}$, caused exclusive nuclear localization similar to that observed in Kip1(1–198) (Fig. 3a), and the fluorescence ratio was significantly lower than that obtained with Kip1R(16–180) (Fig. 3b). On the other hand, the mutation of R166 to I in $p27^{Kip1}$, $Kip1(1–198)^{R166I}$, caused a cytosolic retention similar to that seen with Kip1R(16–180) (Fig. 3a,b). This observation contrasted strongly to that for $Kip1(1–198)^{R166A}$, which caused a distribution similar to that seen with GFP (Fig. 3a), namely, a complete loss of exclusive nuclear localization (Fig. 3b). Furthermore, $Kip1R(16–180)^{I169A}$ significantly increased a degree of cytoplasmic distribution (Fig. 3a,b). The complete removal of basic amino acid while leaving I169 un-mutated, $Kip1R(16–180)^{K168A}$, also caused a significant increase in cytoplasmic distribution (Fig. 3a,b). However, both $Kip1R(16–180)^{I169A}$ and $Kip1R(16–180)^{K168A}$ demonstrated a significantly lower degree of cytoplasmic distribution, namely, significantly higher nuclear localization that that seen with GFP alone (Fig. 3b). The double mutation, $Kip1R(16–180)^{K168A+I169A}$, caused a similar distribution to that seen with GFP alone (Fig. 3a), namely a complete loss of significant nuclear localization (Fig. 3b).

N-Terminal Region Is Prerequisite for Growth Inhibition by Both $p27^{Kip1R}$ and $p27^{Kip1}$

The effects of $p27^{Kip1}$, $p27^{Kip1R}$, and their mutants on the cell growth were evaluated using GFP expression system (Fig. 4). The

growth of the cells with positive and negative expression was evaluated separately based on the total cell count and the transfection rate. When the cells were transfected with GFP alone, $8.2 \pm 0.7\%$ of cells ($n = 3$) were positive for the expression of GFP just after the 5-h transfection period (time 0), and thereafter, the transfection rate increased to the maximum ($62.6 \pm 1.3\%$, $n = 3$) 24 h after transfection (data not shown). Thereafter, the transfection rate did not significantly change until day 5 after transfection (Fig. 4b). On the other hand, the total cell count increased with a doubling time being approximately 24 h (Fig. 4a). Accordingly, the growth rate seen with the GFP-positive cells (Fig. 4c) was similar to that seen with the GFP-negative cells (Fig. 4d) and non-transfected cells (data not shown). On the other hand, when the cells were transfected with Kip1(1–198) and Kip1R(16–180), the transfection rate at time 0 and time to reach a maximum were similar to those observed with GFP alone (data not shown). However, the transfection rates, thereafter, progressively decreased in contrast to the case with GFP alone (Fig. 4b). Accordingly, the expression-positive cells did not increase at all (Fig. 4c), while the expression-negative cells increased similarly to that seen in the transfection with GFP alone (Fig. 4d). The deletion of the N-terminal region containing binding sites for cyclins and Cdks, Kip1(152–198) and Kip1R(152–180), abolished the growth inhibitory activity seen with Kip1(1–198) and Kip1R(16–180), respectively (Fig. 4c,d). Both expression-positive and negative cells in the transfection with Kip1(152–198) and Kip1R(152–180) demonstrated similar growth curves to those seen with GFP alone (Fig. 4c,d). The similarity in the growth rate of the expression-negative cells among different transfections was apparent when the growth rate was evaluated as a fold increase (Fig. 4d, insets).

Western Blot Analysis of Expression of the Recombinant Proteins in HeLa Cells

It is possible that a fluorescence pattern similar to that seen with GFP tag alone was due to free GFP cleaved from fusion protein. To evaluate this point, we examined the expression of the representative truncation and site-directed mutants of $p27^{Kip1}$ and $p27^{Kip1R}$, which showed a similar pattern to that seen with GFP, by a Western blot analysis (Fig. 5). No major free GFP was observed in the cells transfected with

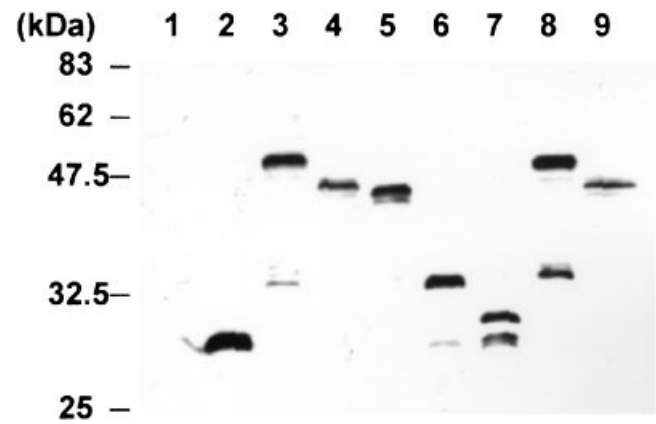

Lane	2	3	4	5	6	7	8	9
Transfection rate (%)	49.7	36.8	36.3	39.8	48.0	42.2	54.8	37.4
Molecular weight (kDa)	26.9	49.7	46.1	44.1	32.6	30.5	49.6	46.0
Relative expression level (%)	263	127	74	104	123	109	93	70

Fig. 5. Western blot analysis of expression of the recombinant proteins in HeLa cells. Chemiluminescence detection of the recombinant proteins in the cells transfected with GFP alone (**lane 2**), Kip1(1–198) (**lane 3**), Kip1R(16–180) (**lane 4**), Kip1/Kip1R(16–162) (**lane 5**), Kip1(154–198) (**lane 6**), Kip1R(155–180) (**lane 7**), $Kip1(1–198)^{R166A}$ (**lane 8**), and $Kip1R(16–180)^{K168A+I169A}$ (**lane 9**). The cell lysate obtained with the non-transfected cells was analyzed as a negative control (**lane 1**). Twenty-microgram total cellular protein was separated on 15% polyacrylamide gel. The GFP fusion proteins were detected with an anti-GFP antibody. The molecular size is indicated on the left. The transfection rate, molecular weight, and the relative expression level compared to the mean expression level obtained with the constructs of $p27^{Kip1}$ and $p27^{Kip1R}$ (lanes 3–9) are shown for each construct.

all constructs, except for Kip1(154–198) and Kip1R(155–180). These two mutants showed a minor cleavage product having a molecular weight similar to that of GFP. The densitometric scan of the chemiluminescence image and the adjustment of the density data according to the transfection rate and molecular weight estimated the molar level of expression of the recombinant protein. The level of GFP was ~2.5-fold of the mean expression level obtained with the constructs of $p27^{Kip1}$ and $p27^{Kip1R}$ (Fig. 5). The expression level of the constructs of $p27^{Kip1}$ and $p27^{Kip1R}$ was within a range between ~70% and ~125% of the mean. The expression level of $p27^{Kip1R}$ mutants containing the residues 16–180 was lower than the average (~70%), while the smaller constructs demonstrated higher level of expression than the average (~120% for Kip1(154–198), ~110% for Kip1R(155–180)).

DISCUSSION

We herein determined the sequences required for nuclear localization and growth inhibition of $p27^{Kip1R}$, and demonstrated the first example of an atypical bipartite NLS with an aliphatic amino acid as a functional residue in $p27^{Kip1R}$ (Fig. 6). This is in strong contrast to the case with $p27^{Kip1}$, which was determined to contain a typical bipartite NLS (Fig. 6). On the other hand, the sequence requirement for growth inhibition by $p27^{Kip1R}$ was identical to that seen with $p27^{Kip1}$. The N-terminal region common to both isoforms was determined to be responsible for growth inhibition. Since the molecular mass of GFP fusion proteins used in the present study was no greater than 50 kDa, their subcellular localization is considered to be determined by a balance between active nuclear transport and passive diffusion. When NLS maintained its full activity as in Kip1(1–198), passive cytoplasmic diffusion appeared to be masked by a active nuclear import at the equilibrated state, and the protein was exclusively localized in the nucleus. On the other hand, a complete loss of NLS eliminated active nuclear import, but did not cause an exclusion of GFP fluorescence from the nuclei because of passive diffusion. The attempts to trap the mutants missing functional NLS in the cytoplasm by adding one or two more GFP tags or a fragment of bovine serum albumin were unsuccessful (data not shown). We therefore quantitatively evaluated the subcellular localization with a single GFP tag. The subcellular distribution thus varies from an exclusive nuclear localization to the distribution similar to GFP. The latter pattern was considered to indicate a complete loss of significant nuclear localization. The Western blot analysis ruled out the possibility that such fluorescence pattern was due to free GFP.

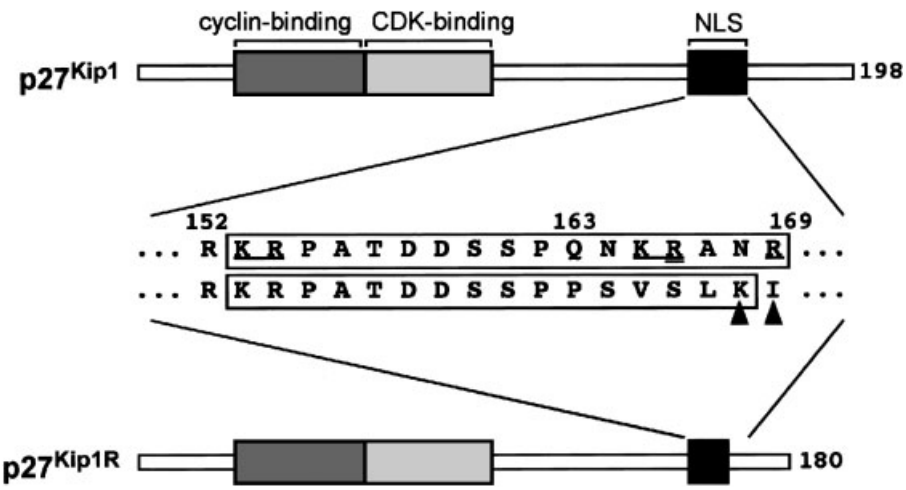

Fig. 6. Comparison of the sequences required for the nuclear localization between $p27^{Kip1}$ and $p27^{Kip1R}$. A structure of $p27^{Kip1}$ and $p27^{Kip1R}$ is schematically shown, and the amino acid sequences required for nuclear localization are indicated. In $p27^{Kip1}$, the region required for the full activity of the nuclear localization signal is boxed, and the basic amino acids, which play a critical role in nuclear localization, were underlined. The double underlined residue, R166, indicates the most important residue in determining the nuclear localization in $p27^{Kip1}$. In $p27^{Kip1R}$, the minimal sequences required for a significant nuclear localization is boxed, and the residues required for nuclear localization in the C-terminal region specific to $p27^{Kip1R}$ are indicated by arrowheads.

The region 153–169 of $p27^{Kip1}$ was determined to be necessary for the full activity of NLS. We previously reported the region 153–166 to be a minimal sequence required for a significant nuclear localization, while its activity as NLS was significantly attenuated [Zeng et al., 2000]. The present study advanced previous observations and revealed that the extension of 3 residues to R169 was required to obtain the full activity of NLS. However, the residue R166 was confirmed to be the most important residue in determining nuclear localization. This configuration of the NLS in $p27^{Kip1}$ (KRPATDDSSPQN-KRANR) perfectly matches the consensus sequence of a bipartite NLS. The typical bipartite NLS is composed of two basic residues at the N-terminus, followed by 10–12 residues of the spacer region and 3–4 basic residues out of C-terminal 5 residues [Dingwall and Laskey, 1991; Conti et al., 1998]. On the other hand, the region 153–168 of $p27^{Kip1R}$ required for the nuclear localization thus only partly fulfill this consensus sequence. In particular, the C-terminal region specific to $p27^{Kip1R}$ contains only one basic amino acid, R168. The inclusion of this residue, Kip1R(1–168), caused a significant nuclear localization, while its nuclear localization was also greatly impaired. The extension to G170 showed a similar nuclear localization to that seen with Kip1R(1–168). As a result, the region 153–168 is concluded to be the minimal sequence required to obtain a significant nuclear localization of $p27^{Kip1R}$. However, the nuclear localization of $p27^{Kip1R}$ was very susceptible to truncation in contrast to the case with $p27^{Kip1}$, probably due to the weak NLS in $p27^{Kip1R}$. It is thus difficult to clearly delineate the boundary of the NLS in $p27^{Kip1R}$.

The most important finding in the present study was that aliphatic amino acid substitutes some functional role of basic amino acid in the NLS. The most critical evidence is that the mutation of R166 to I in $p27^{Kip1}$ significantly but slightly attenuated the nuclear localization, thus causing a cytoplasmic distribution similar to that seen with $p27^{Kip1R}$. However, the mutation of R166 to A caused a complete loss of nuclear localization. On the other hand, the mutation of I169 to R in $p27^{Kip1R}$ caused an exclusive nuclear localization similar to that seen with $p27^{Kip1}$, while the mutation of I169 to A caused further reduction of nuclear localization. The cluster K168–I169 in $p27^{Kip1R}$ was thus suggested to functionally correspond to the cluster K165–R166 in $p27^{Kip1}$, in addition to the fact that both clusters contain the first basic residue following the spacer region of the bipartite NLS (Fig. 6). It is thus concluded that aliphatic amino acid can substitute for basic amino acid in the bipartite NLS. However, its functional substitution was incomplete and thereby caused a reduced activity in the NLS and cytoplasmic retention as seen with $p27^{Kip1R}$.

There have been several reports on the atypical bipartite NLS [Gugneja et al., 1996; Gallay et al., 1997; Brownawell et al., 2001]. A transcription factor NRF-1 contains an atypical NLS consisting of functionally redundant clusters of basic residues [Gugneja et al., 1996]. Integrase, one of the HIV-1 nucleoprotein complexes, contains an atypically long spacer region consisting of 22 amino acids [Gallay et al., 1997]. In a forkhead transcription factor AFX, a stretch of 42 amino acids containing 12 basic residues was shown to serve as a NLS, but its sequences do not fit to any classical types of NLS [Brownawell et al., 2001]. In $p27^{Kip1R}$, the spacer region consists of 13 amino acids, and is thus a little longer than the consensus sequences. However, the most striking feature in $p27^{Kip1R}$ is that a putative NLS is missing a number of basic residues and instead utilizes an aliphatic amino acid. $p27^{Kip1R}$ is the first example of an atypical NLS with an aliphatic amino acid as a functional residue.

The cytoplasmic localization of $p27^{Kip1R}$ is considered to result from an atypical NLS with a reduced activity due to a substitution of a basic residue by an aliphatic amino acid. However, the functional significance of the cytoplasmic retention of $p27^{Kip1R}$ due to the distinct C-terminus remains to be investigated. In the present study, the N-terminal but not C-terminal region of both $p27^{Kip1}$ and $p27^{Kip1R}$ was determined to be linked to the growth inhibition. Furthermore, the growth inhibitory effect of $p27^{Kip1}$ and $p27^{Kip1R}$ was not due to the expression of GFP protein, because the growth rate (Fig. 4) and the cell cycle profile [Hirano et al., 2001a] of the cells expressing GFP alone were similar to those seen not only with the GFP-negative cells obtained in the same transfection but also with the non-transfected cells. Both truncation mutants, Kip1(152–198) and Kip1R(152–180), exerted no inhibitory effect on cell growth, while they retained their ability to localize in the nucleus. These results indicated

that the growth inhibition induced by $p27^{Kip1}$ and $p27^{Kip1R}$ appears to originate in the N-terminal region, and it is not just related to their nuclear localization. The C-terminal region has been suggested to include a different function from that carried by the N-terminal region [Nagahara et al., 1998]. In HepG2 cells, the N-terminal region was reported to be sufficient for G_1 arrest, while the C-terminal region was necessary to induce cell-scattering and filopodia formation [Nagahara et al., 1998]. In order to characterize the different roles of these two isoforms, the function related to the C-terminal region specific to each isoform remains to be elucidated.

In conclusion, the regions 153–168 and the residue I169 are thus considered to play a critical role in the nuclear localization of $p27^{Kip1R}$. This configuration is not a typical bipartite NLS due to the fact that the C-terminal part contains only one basic amino acid and that an aliphatic amino acid is utilized in place of a basic residue. The functional substitution by an aliphatic residue is incomplete, thereby causing a cytoplasmic retention of $p27^{Kip1R}$. Despite a significant cytoplasmic retention, $p27^{Kip1R}$ inhibited the growth of HeLa cells as well as $p27^{Kip1}$. The growth inhibition by $p27^{Kip1}$ and $p27^{Kip1R}$ is thus concluded to originate in the N-terminal region, and such inhibition is not just related to their nuclear localization.

ACKNOWLEDGMENTS

We thank Mr. Brian Quinn for linguistic comments and help with the manuscript. This study was supported in part by Grants-in-Aid for Scientific Research (No. 13557067, 13470149, 13832006, 13671591, 13670723) and for Scientific Research on Priority Area (No. 13214077) from the Ministry of Education, Culture, Sports, Science and Technology, Japan, by Research Grants for Cardiovascular Diseases (11C-1, 12C-2, 13C-4) from the Ministry of Health, Labour and Welfare, Japan, and by grants from the NOVARTIS Foundation (Japan) for the Promotion of Science, the Japan Space Forum, and the Mochida Memorial Foundation for Medical and Pharmaceutical Research.

REFERENCES

Brownawell AM, Kops GJ, Macara IG, Burgering BM. 2001. Inhibition of nuclear import by protein kinase B (Akt) regulates the subcellular distribution and activity of the forkhead transcription factor AFX. Mol Cell Biol 21:3534–3546.

Conti E, Uy M, Leighton L, Blobel G, Kuriyan J. 1998. Crystallographic analysis of the recognition of a nuclear localization signal by the nuclear import factor karyopherin alpha. Cell 94:193–204.

Dingwall C, Laskey RA. 1991. Nuclear targeting sequences—A consensus? Trends Biochem Sci 16:478–481.

Gallay P, Hope T, Chin D, Trono D. 1997. HIV-1 infection of nondividing cells through the recognition of integrase by the importin/karyopherin pathway. Proc Natl Acad Sci USA 94:9825–9830.

Gugneja S, Virbasius CM, Scarpulla RC. 1996. Nuclear respiratory factors 1 and 2 utilize similar glutamine-containing clusters of hydrophobic residues to activate transcription. Mol Cell Biol 16:5708–5716.

Hirano K, Hirano M, Zeng Y, Nishimura J, Hara K, Muta K, Nawata H, Kanaide H. 2001a. Cloning of a degradation-resistant isoform of $p27^{Kip1}$. Biochem J 353: 51–57.

Hirano M, Hirano K, Nishimura J, Kanaide H. 2001b. Transcriptional up-regulation of $p27^{Kip1}$ during the contact-induced growth arrest in the vascular endothelial cells. Exp Cell Res 271:356–367.

Ho SN, Hunt HD, Horton RM, Pullen JK, Pease LR. 1989. Site-directed mutagenesis by overlap extension using the polymerase chain reaction. Gene 77:51–59.

Kalderon D, Roberts BL, Richardson WD, Smith AE. 1984. A short amino acid sequence able to specify nuclear location. Cell 39:499–509.

Nagahara H, Vocero-Akbani AM, Snyder EL, Ho A, Latham DG, Lissy NA, Becker-Hapak M, Ezhevsky SA, Dowdy SF. 1998. Transduction of full-length TAT fusion proteins into mammalian cells: TAT-$p27^{Kip1}$ induces cell migration. Nat Med 4:1449–1452.

Polyak K, Lee MH, Erdjument-Bromage H, Koff A, Roberts JM, Tempst P, Massague J. 1994. Cloning of $p27^{Kip1}$, a cyclin-dependent kinase inhibitor and a potential mediator of extracellular antimitogenic signals. Cell 78: 59–66.

Russo AA, Jeffrey PD, Patten AK, Massague J, Pavletich NP. 1996. Crystal structure of the $p27^{Kip1}$ cyclin-dependent-kinase inhibitor bound to the cyclin A-Cdk2 complex. Nature 382:325–331.

Sherr CJ, Roberts JM. 1995. Inhibitors of mammalian G1 cyclin-dependent kinases. Genes Dev 9:1149–1163.

Toyoshima H, Hunter T. 1994. p27, a novel inhibitor of G1 cyclin-Cdk protein kinase activity, is related to p21. Cell 78:67–74.

Zeng Y, Hirano K, Hirano M, Nishimura J, Kanaide H. 2000. Minimal requirements for the nuclear localization of $p27^{Kip1}$, a cyclin-dependentkinase inhibitor. Biochem Biophys Res Commun 274:37–42.